Proceedings of the Fourth
Interagency Meeting on Cryocoolers
Plymouth, MA (1990)
David Taylor Research Center DTRC-91/003 (1991)

DEVELOPMENT OF A THERMOACOUSTICALLY DRIVEN ORIFICE PULSE TUBE REFRIGERATOR*

Ray Radebaugh and K.M. McDermott
National Institute of Standards and Technology
Boulder, Colorado 80303

G.W. Swift and R.A. Martin
Los Alamos National Laboratory
Los Alamos, New Mexico 87545

ABSTRACT

The project to develop a thermoacoustically driven orifice pulse tube refrigerator (TADOPTR) was started in February 1989 to meet the infrared sensor cooling requirements of Strategic Defense Initiative Office (SDIO) satellite programs. It is a cooperative effort involving development of a thermoacoustic driver (TAD) by Los Alamos National Laboratory (LANL) and development of an orifice pulse tube refrigerator (OPTR) by the National Institute of Standards and Technology (NIST). The heat-driven TAD provides a 28 Hz oscillating, thermoacoustically-produced pressure source for the OPTR, eliminating the need for a mechanical compressor. The TADOPTR is the first cryocooler with no moving parts; thus, it has potential for exceptional reliability and low cost. The first laboratory model built to test the concept achieved a low temperature of 90 K with no load and produced 5 W of cooling power at 120 K. The TAD was powered by an electrical heater at temperatures up to 965 K. This paper documents the design, fabrication, and performance of the first TADOPTR, and states developmental goals for the future.

INTRODUCTION

One important requirement of cryocoolers intended for cooling infrared sensors on satellites is high reliability. Desired lifetimes are usually in the range of 5 to 10 years. Much of present cryocooler research and development is focused on developing methods for achieving high reliability. Stirling refrigerators are being studied extensively for this application with anticipation that they will achieve both high reliability and efficiency.

---

*Research sponsored by the Sensors Office of the Strategic Defense Initiative Organization (SDIO).

Because Stirling refrigerators require two moving parts, a piston and a displacer, costly support mechanisms need to be developed to allow the parts to move without contacting the stationary cylinder walls. Costly clearance seals with precise tolerances of 10 to 15 μm are also required.

An alternative approach to achieving high reliability involves eliminating the moving parts altogether. The functions of the displacer and piston can be replaced by the working fluid itself. The orifice pulse tube refrigerator (OPTR) is a variation of the Stirling refrigerator in which a gas column in a tube replaces the solid displacer of the Stirling refrigerator.[1,2] Figure 1 shows a schematic of the OPTR. Proper phasing of the motion of the gas segment is caused by the flow of warm gas through the orifice, which is in phase with the oscillating pressure. Previously, the pressure oscillation required to drive the OPTR was produced by a separate mechanical compressor.

To eliminate the one remaining moving part, the compressor has been replaced with a thermoacoustic driver (TAD), shown schematically in Figure 2. Pressure oscillations in the TAD occur when the working gas experiences an oscillating flow of heat between it and a stationary matrix of closely spaced plates (called the "stack"). The oscillating heat flow occurs when the gas parcels oscillate along a steady temperature gradient in the stack; the temperature gradient is brought about by a constant heating rate at one end of

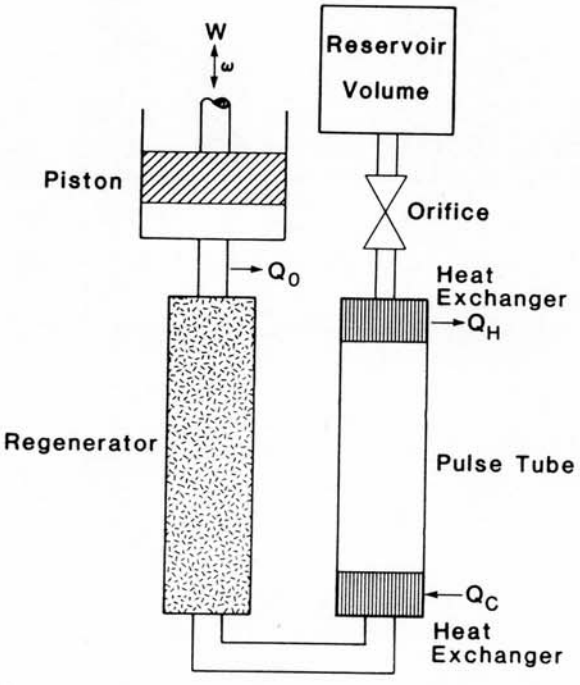

Fig. 1. Schematic of the OPTR, in which the piston is the only moving part.

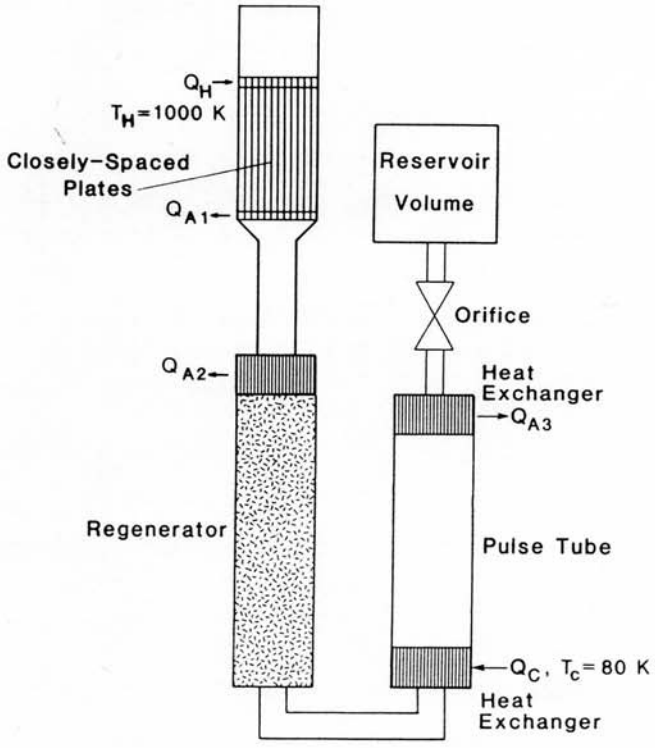

Fig. 2. Schematic of the TADOPTR, which has no moving parts.

the stack and cooling at the other end. Because the pressure and the gas motion through the temperature gradient are coupled in the closed system, self-driven pressure oscillations occur whenever the temperature gradient in the stack exceeds a critical value. The pressure oscillations occur in the form of an acoustic standing wave.

Combining the TAD with the OPTR yielded the thermoacoustically driven orifice pulse tube refrigerator (TADOPTR), producing cryogenic refrigeration with no moving parts.

Wheatley and Cox[3] reported on a related device in which a TAD was used to drive a resonant pulse tube refrigerator (thermoacoustic refrigerator). They achieved a low temperature of 262 K, well above the cryogenic range (defined as temperatures below 120 K). As pointed out by Radebaugh,[1] the OPTR is a much more powerful refrigerator than the thermoacoustic refrigerator. Consequently, the first demonstration model of the TADOPTR achieved a temperature of 90 K, making it the first cryogenic refrigerator with no moving parts. Two problems which had to be overcome in order to achieve this high performance were the reduction of the resonance frequency of the TAD to a value needed for the OPTR (below 30 Hz), and the operation of the OPTR at low pressure ratios (ratio of pressure maximum to pressure minimum below 1.1).

THERMOACOUSTIC DRIVER DEVELOPMENT

TAD DESCRIPTION AND REQUIREMENTS

The TAD is a resonant, heat-driven compressor with no moving parts, designed specifically to compress helium gas in the OPTR. Only the working gas moves in the TAD. There are no sliding or rotating parts to seal; hence, there are no exacting tolerances. The TAD is a simple, robust, exceptionally reliable, direct energy conversion device. Thermodynamic cycle efficiencies of 15% to 30% (20% to 40% of Carnot's ideal efficiency) are expected for the TAD.

The TAD was designed to produce oscillations at 27 Hz; as a result, a relatively long resonator tube was needed. A schematic of the TAD with the OPTR connected to it is shown in Figure 3 and a photograph of the system, in Figure 4. The 3.05 m diameter loop in these figures is part of the TAD.

Discussions between NIST and LANL scientists resulted in preliminary design goals. Under idealized conditions, 1 kW of heat would be input through the hot-end heat exchangers of the TAD at a temperature of 1000 K. The heat source could be electrical, solar, or nuclear. (A number of compact heater units[4] powered by radioisotopes and capable of producing more than 1 kW of heat have already flown in space as part of radioisotope thermal generator (RTG) systems.) The TAD compressor thermoacoustically converts a portion of this heat (about 25%, or 250 W) to acoustic power inside the stack and rejects the balance as waste heat in heat exchangers at ambient temperature. Preliminary estimates predicted that about 185 W of the 250 W of acoustic power would be consumed by viscous and compressive losses inside the resonator. The remaining

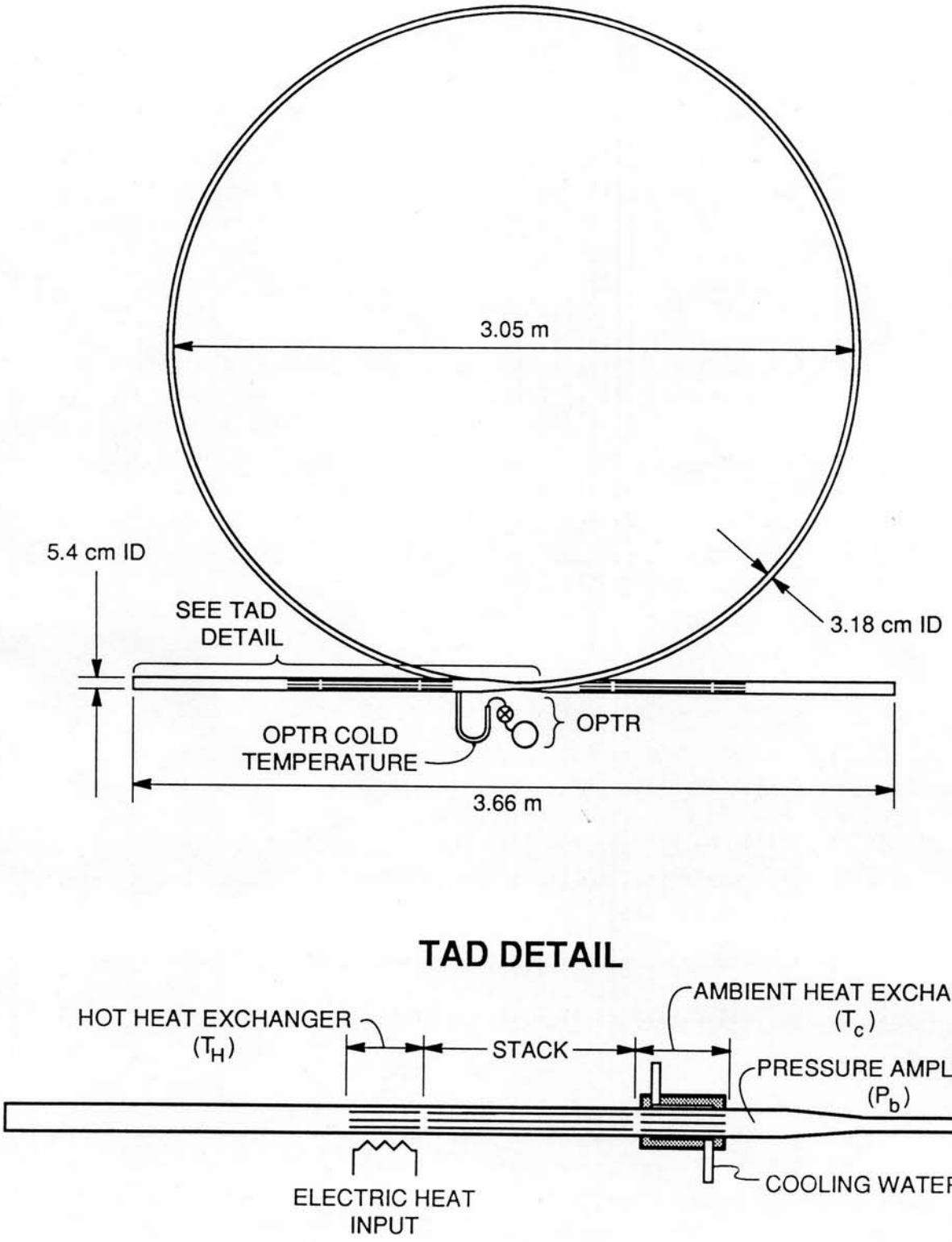

Fig. 3. Schematic of TADOPTR. Shown in the upper diagram is the TAD resonator, housing two heat exchangers and one stack per engine. Details for one engine are shown in the lower diagram.

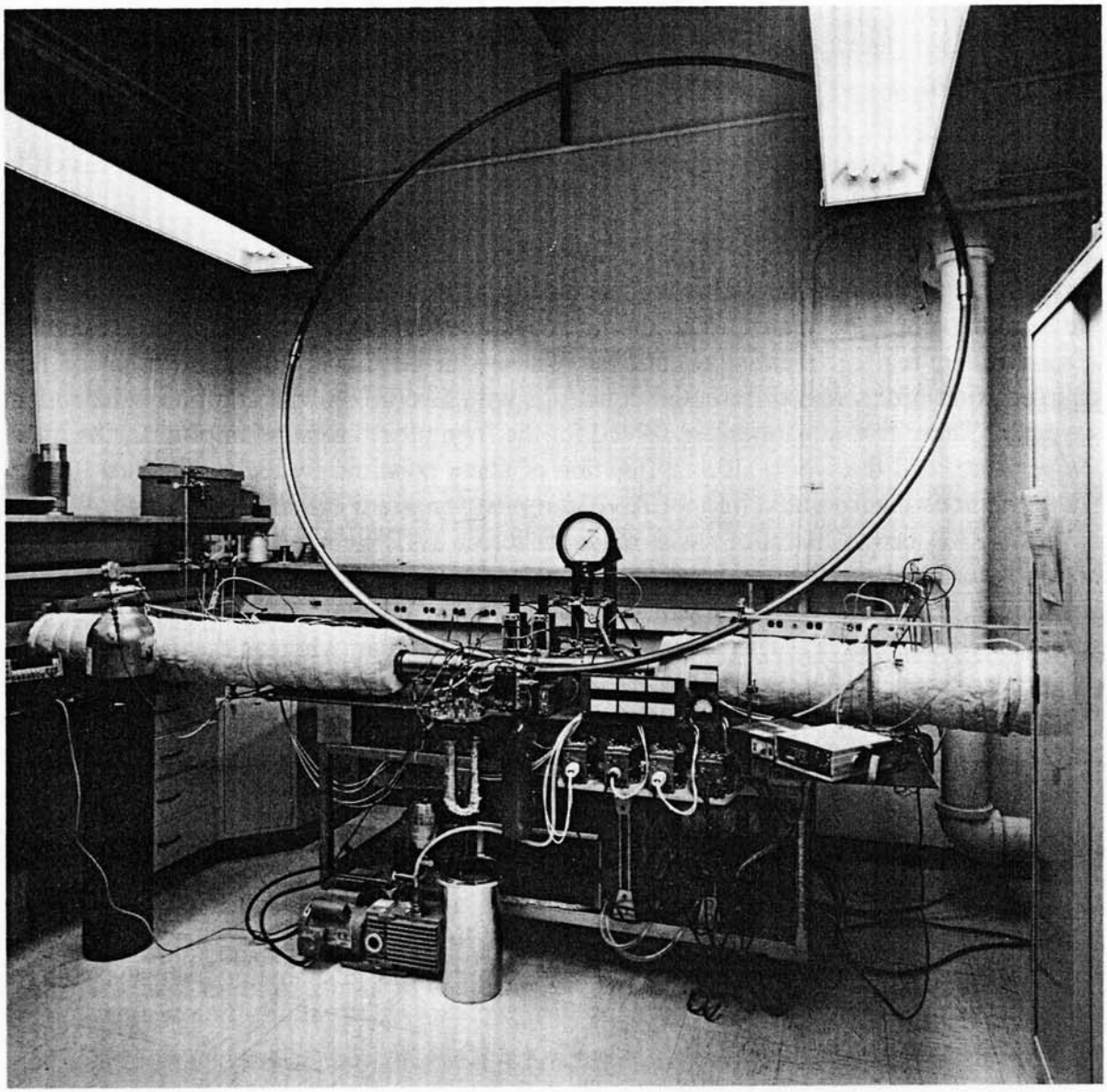

Fig. 4. Photograph of the TADOPTR. The TADs are inside the heavy white insulation; the large loop forms the rest of the resonator. The OPTR is the U-shaped tube just left of the center.

65 W would be available to power the OPTR.

The expected pressure oscillations of 250 kPa zero-to-peak amplitude, found near the ambient heat exchangers along the standing wave in the TAD resonator, would be used to drive the OPTR. While the pressure amplitude is about 6% higher at the hot end of the resonator case, a lower amplitude was accepted in order to connect the devices at 300 K instead of 1000 K.

THERMOACOUSTIC THEORY AND APPLICATION TO TAD

Swift[5] has written a comprehensive review paper that presents the fundamentals of thermoacoustic engine theory and design. It rigorously presents many assumptions which underlie the theory used to design the TAD and provides examples of thermoacoustic engine design. This paper should be the starting point for anyone seriously interested in pursuing the subject.

A general thermoacoustic theory evolved from applying the laws of conservation of mass, momentum, and energy, as well as equations of state and thermophysical data for the working fluid and plates. The thermoacoustic equations are a set of three coupled, second-order, real differential equations. These can be transformed into a set of five coupled, first-order, real differential equations with five unknowns and one independent variable. These five equations are solved for the (complex) pressure amplitude, the mean temperature, and the work, all as a function of stack position, by using standard Runge-Kutta methods incorporated into a LANL computer program called WAVTAD. A series of WAVTAD design iterations was made to select TAD geometric parameters, and to obtain theoretical predictions for TAD performance. The most efficient design (i.e.,the least heat input for a given acoustic power) was selected for fabrication, and is summarized in Table 1. The values are for a single engine, whereas the TAD uses two of these engines. WAVTAD predicted that a total of 2600 W of heat would be required to drive the TAD at a pressure amplitude of 250 kPa, supplying 388 W of acoustic power to the OPTR. These design goals were not achieved during actual operation of the TADOPTR; this is discussed in more detail later.

TAD DESIGN, FABRICATION, AND SPECIFICATIONS

As shown in Figures 3 and 4, the TAD consists of two identical engines that share a common resonator. The resonator is the 3.05 m diameter loop between the two 1.83 m straight, horizontal segments on the bottom. A reduction in diameter from the straight segments to the central portion shortens the resonator substantially below one-half an acoustic wavelength[5] of 27 Hz.

One of the two thermoacoustic engines is shown schematically in more detail at the bottom of Figure 3. The hot end of the resonator casing consists of Schedule 160 stainless steel pipe, containing a heat exchanger with closely spaced parallel copper plates and a thermoacoustic stack constructed of closely spaced stainless steel plates and spacers (see Table 1). Flexible electrical heating elements, wound around the steel pipe, were

Table 1. TAD single engine performance as predicted by WAVTAD.

Resonator frequency	27 Hz
Stack plate half-spacing	0.5 mm
Stack plate half-thickness	0.06 mm
Hot temperature	1000 K
Stack distance from closed end	0.75 m
Stack length	1.00 m
Pressure amplitude, P_1	250 kPa
Mean pressure, P_0	3040 kPa
Input heat rate	1300 W
Stack diameter	5.08 cm
Cold temperature	300 K
Acoustic power	403 W
Efficiency	0.31
Efficiency/Carnot efficiency	0.44
Dissipation in half of resonator	209 W
Power available for OPTR	194 W

used to heat the hot-end heat exchanger. Power to the heating elements was controlled using variable autotransformers. The entire hot section was insulated with a high-temperature alumina-silica blanket.

Each ambient heat exchanger had a similar parallel plate construction and was cooled on the outside by an annular water jacket, using a metered water flow rate of 32 cm^3/s. The heat exchanger was connected to the hot section using a flange, and to the resonator loop by a brass transition section, also using flanges. The heat exchanger and stack parts were brazed or soft-soldered together in rectangular parallelepiped billets, and were then cut into cylindrical shapes using wire electric-discharge machining. More complete details of dimensions and construction techniques are available on request.

TAD INSTRUMENTATION

All components of the TAD were instrumented to obtain performance data. Eighteen thermocouples were used both to determine when steady-state operating conditions were achieved and to measure the axial temperature gradients. Four more thermocouples were mounted inside the two hot-end heat exchangers to measure the temperature of the working gas and the radial temperature gradients. The average of the readings from two of these four thermocouples defined the hot temperature. Power input to the electric heaters was determined from the voltage and current output of the variable autotransformer.

To calculate waste heat removal at the ambient heat exchangers, which allowed heat

balance and efficiency to be checked, the cooling water flow rates and temperature increases were measured with flowmeters and differential temperature sensors. In addition, the absolute temperature of the cooling water was measured with an immersed thermocouple.

Oscillating pressure amplitude was measured in the resonator at symmetrical locations on either side of the TAD using piezoelectric pressure transducers. Absolute mean pressure of the helium gas was measured using a Bourdon-tube pressure gauge.

RESULTS OF PRELIMINARY TAD EXPERIMENTS

The TAD was initially tested without the OPTR. Tests were conducted at a mean pressure of 3.1 MPa. The objectives were to compare TAD performance to theoretical predictions before connecting it to the OPTR, to gain operating experience with the new engine, to confirm repeatability and constancy of performance, and to demonstrate reliability and longevity.

The TAD produced acoustic power at the design frequency (27 Hz at low amplitude and 28 Hz at high amplitude) the first time it was turned on. It has operated without a single failure and has needed no maintenance up to the present. The TAD has been started and shut down approximately 100 times without failure, both with and without the OPTR. Over this one year period, the hot-section temperatures for a given input power were repeatable within a few kelvins, and the pressure amplitudes were repeatable within 1%. Pressure typically began to oscillate within one hour of startup from ambient (cold) conditions. Oscillographic recordings of the thermocouple temperature readings were used to confirm steady-state operation before taking data.

Testing the TAD without a load produced relative pressure ratios of P_1/P_0 (pressure amplitude/mean pressure) up to 0.048, which corresponds to a high-to-low pressure ratio, P_H/P_L, of 1.10. The total electrical input to the TAD was 2026 W, which produced a hot temperature of 668 K. Data from this test are included in the zero-load measurements in Figure 5, which shows the dependence of the square of the TAD pressure amplitude and of hot-end temperature on heat input. Also shown in Figure 5 are the theoretical (calculated) curves for these quantities. The acoustic power produced by the TAD is proportional to the square of the pressure amplitude. This figure indicates that the predicted value of the no-load pressure amplitude is considerably higher, and that of the hot-end temperature lower, than the measured values. For example, at a heat input of 2026 W, the calculated value for $(P_1/P_0)^2$ is 0.0058, which is higher than the measured value of 0.0023 by a factor of 2.5. In addition, the calculated hot temperature of 600 K is 67 K lower than the measured value of 667 K. Because thermoacoustic power production and the internal loss mechanisms are both proportional to P_1^2, the theory predicts a constant value for the stack temperature gradient after heating to the critical value. In contrast, the data show a linear increase in the temperature gradient, probably reflecting resonator losses increasing faster than P_1^2.

The calculated and measured performance data for tests with the OPTR connected are

also shown in Figure 5. This figure shows that the OPTR absorbed power from the TAD and that the temperature gradient across the stack increased, as predicted, but there is disagreement between the magnitudes of the calculated and measured data. Possible causes of this are being investigated at LANL. Part of the performance disagreement is due to larger heat losses through the insulation at the hot end of the TAD than first estimated. Also, the theoretical model was developed for an infinite parallel plate geometry in the stack, while the flow passages in the TAD have rectangular cross-sections with an aspect ratio of about 10 to 1. For oscillatory flow conditions, turbulence is

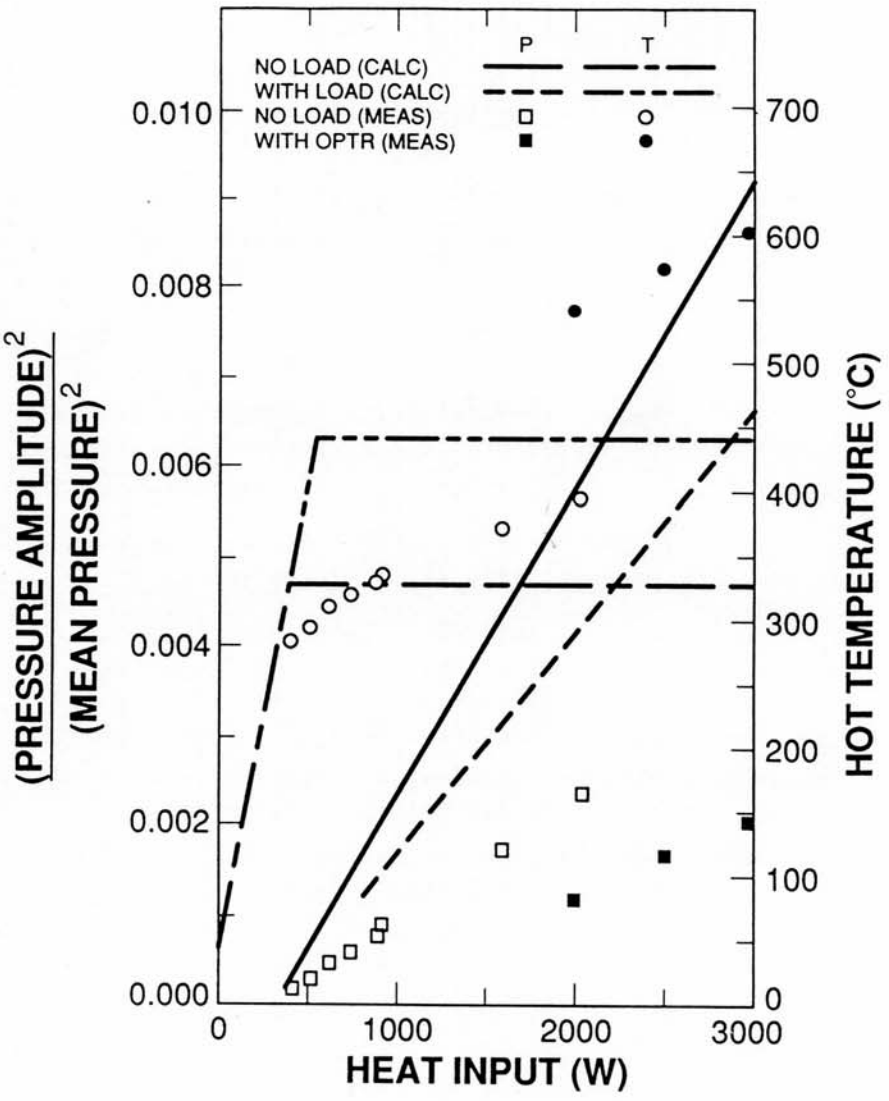

Fig. 5. Graphs of calculated and measured TAD performance with and without the OPTR connected. Comparisons of both $(P_1/P_0)^2$ and hot temperature performance are made.

possible at the entrance and exit of the heat exchangers; this is not accounted for in the linear acoustics theory. Furthermore, because of the radial temperature gradients in the heat exchangers, it is thought that a convective heat transfer phenomenon known as "acoustic streaming"[6] may be degrading performance in the TAD; other thermoacoustic engines built to date have exhibited similar discrepancies. These losses are not included in this theory, which considers only first-order viscous losses and thermal dissipation at the surfaces. Increased losses in the small-diameter section of the resonator, where large-displacement, high-velocity flow occurs at high Reynolds numbers (as high as 10^6, with Mach numbers as high as 0.2) are also not accounted for.

ORIFICE PULSE TUBE REFRIGERATOR DEVELOPMENT

OPTR THEORY AND DESIGN

The theory of the OPTR has been discussed in several papers by Radebaugh, et al.[2,7] The normalized gross refrigeration power G is given by[2]

$$G = \dot{Q}_c / [\langle \dot{m}_c \rangle RT_c \ln(P_H/P_L)] = (\pi/8)\cos\theta, \quad (1)$$

where $\dot{Q}_c$ is the gross refrigeration power, $\langle \dot{m}_c \rangle$ is the mass flow rate at the cold end averaged over one half cycle, R is the gas constant per unit mass, T_c is the cold temperature, and θ is the phase angle between the mass flow rates at each end of the pulse tube. For $\theta=30°$, G is 0.34, while experimentally G has been found[8] to be about 0.075. The term $\langle \dot{m}_c \rangle$ can be related to the pulse tube volume by the expression

$$\langle \dot{m}_c \rangle = 4f(P_1/P_0)P_0V_t / \gamma RT_c \sin\theta, \quad (2)$$

where f is the frequency, V_t is the pulse tube volume, and γ is the ratio of specific heats.

Because of the low pressure ratio produced by the TAD, the refrigeration power per unit mass flow rate will be quite low according to Equation (1); thus, regenerator losses can significantly degrade regenerator performance. To design the regenerator for the OPTR, a computer program developed at NIST called REGEN/REGEN2 was used; this model neglects the effect of regenerator void volume. For a flow rate of 4.1 g/s (P_H/P_L=1.10, P_0=3.1 MPa) in a regenerator with dimensions given in Table 2, the regenerator loss calculated by REGEN2 was 2.6 W and the calculated conduction loss was 0.9 W. The net refrigeration power was 3.7 W at 120 K for a 51.9 cm^3 pulse tube with dimensions shown in Table 2. The relative pressure drop $\Delta P/P_0$ in the regenerator was calculated to be 0.0054.

The heat exchanger on the warm end of the pulse tube must be capable of dissipating the gross refrigeration power of 7.2 W. The heat exchanger on the warm end of the regenerator must be able to remove an incoming enthalpy flow from the TAD of 50 W

or more.

OPTR CONSTRUCTION

A cryostat, which is a stainless steel vacuum can, surrounds the heat exchangers, the regenerator, and the pulse tube, shown in Figure 6. The needle valve (orifice) and the 2700 cm^3 reservoir volume are located outside the cryostat. Radiative heat loss to the low temperature sections is reduced by wrapping both the regenerator and the lower 80% of the pulse tube with approximately 20 layers of aluminized Mylar. During normal operation the vacuum in the cryostat is maintained below 10^{-3} Pa (10^{-5} torr).

The regenerator was made from a 304 stainless steel tube with dimensions shown in Table 2. The regenerator diameter is large since the pressure drop must be kept very low to utilize the low pressure amplitude produced by the TAD. The regenerator matrix was made by stacking 2000 layers of 200-mesh (0.127 mm spacing) stainless steel screen into the tube. Due to the flexibility of the screen and the relatively large diameter of the tube, one 80-mesh (0.32 mm spacing) stainless steel screen was inserted after every 30 to 50 mm of the finer screen. This reinforcement prevented bowing of the 200-mesh screen as it was packed. Bowing results in the edges of the screen pulling away from the tube wall, causing channeling of the flow to the annular space between the wall and the mesh.

The pulse tube was made from a 304 stainless steel tube; its dimensions are shown in Table 2. A stainless steel flange was vacuum-brazed to the hot end, and a copper fitting was vacuum-brazed to the cold end. This copper fitting contained about 30 layers of 80-mesh copper screen to serve as both a flow straightener and a heat exchange surface to enhance heat transfer between the heat load and the working fluid.

The heat exchangers are attached to the hot ends of both the regenerator and the pulse tube to fix the warm-end temperatures. Copper screen of 80-mesh was used for the internal matrix of both heat exchangers. Figure 6 shows a cross-section of the heat exchangers, pulse tube, and regenerator. Water cooling was used for both warm-end heat exchangers. The void volume of the gas in the regenerator heat exchanger is 15.2 cm^3, and in the pulse tube heat exchanger it is 3.5 cm^3.

Table 2. Parameters for the regenerator and pulse tube.

	Outside diameter (mm)	Wall thickness (mm)	Length (mm)	Screen	Porosity	Gas vol. (cm^3)
Regenerator	41.28	0.89	208	200-mesh S.S.	0.69	175.8
Pulse tube	19.05	0.51	203	N/A	N/A	51.9

The orifice is an 11-turn needle valve having an orifice diameter of 3.18 mm. Optimum orifice settings ranged from about 1 turn for no heat load, to 3 turns with a heat load of 5 W.

OPTR INSTRUMENTATION

The experimental values measured were the temperature at both the cold and warm ends of the pulse tube, the heat input to the cold end of the pulse tube, the heat rejection at the warm end of the pulse tube and regenerator, and the instantaneous pressures at the warm ends of the pulse tube and regenerator. Temperatures are measured with diode thermometers that have an accuracy of ± 0.5 K. The heater at the cold end of the pulse tube is a resistance heater. Power input was determined by measuring the current into the

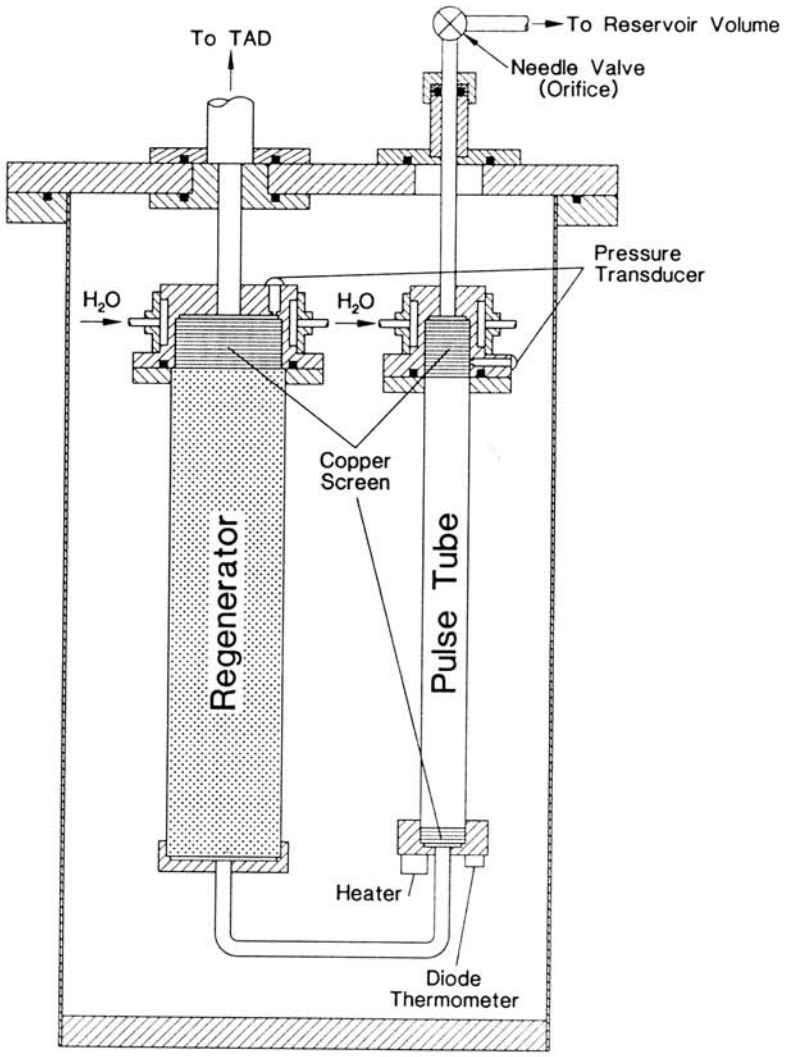

Fig. 6. Cross-sectional view of the various OPTR components and transducers.

heater, which has a known resistance. This measurement was accurate to less than 1%. Instantaneous pressures were measured with piezoresistive pressure transducers responding to frequencies from d.c. to about 500 kHz. The combined nonlinearity, non-repeatability, and pressure hysteresis are less than 0.5% of full scale. Pressure oscillations were monitored on a 4-channel digital oscilloscope and could be observed simultaneously. To compare the behavior of the piezoresistive pressure transducers used in the OPTR with the piezoelectric pressure transducers used in the TAD, one of the piezoresistive and two of the piezoelectric transducers were temporarily mounted close to each other at the point where the OPTR was connected to the TAD. The measured pressure amplitudes from all three transducers agreed within 1%.

To measure the heat rejected to the flowing water by the heat exchangers at the warm ends of both the pulse tube and regenerator, an electrical heater was placed downstream from each heat exchanger. If the temperature increase of the water passing through the heater is made equal to the temperature increase as it passes through the heat exchanger, the heat input to the heater is equal to the heat rejected by the heat exchanger. This assumes the temperature changes are small enough so that the change in the specific heat of the water is negligible. A special three-legged thermopile was designed that has a zero voltage output when the two temperature increases are equal.

TADOPTR RESULTS

The OPTR was attached to the TAD on October 25, 1989, and heat was applied to the TAD the following day. Immediately after the pressure oscillations began, the temperature of the pulse tube started decreasing. The lowest temperature achieved by the TADOPTR was 90 K, after the orifice was adjusted for minimum temperature. The refrigeration power of the TADOPTR is shown in Figure 7 for three different power inputs to the TAD. The warm-end temperatures of the regenerator and pulse tube were approximately 290 K for all of these measurements. The heat rejected in the heat exchangers, with 3 kW of heat applied to the TAD and 5 W applied to the OPTR, was 15 W at the pulse tube and 70 W at the regenerator. Temperatures and pressure ratios in the TADOPTR are shown in Table 3. The experimental net refrigeration power of 5 W at 120 K exceeds the calculated value of 3.7 W, even for the lower observed pressure ratio of 1.05 in the pulse tube (compared to 1.10, which was used for the calculation). Figure 8 shows the pressures (i) in the TAD next to the OPTR connection, (ii) at the entrance to the warm heat exchanger above the regenerator, and (iii) at the warm end of the pulse tube. Notice the distortion of the waveform in the pulse tube as opposed to the nearly sinusoidal behavior at the other two locations. This distortion may be due to a nonlinear flow through the orifice or due to rapid temperature swings in the pulse tube. The pressure ratios in the pulse tube were all about 1.05. The corresponding relative pressure amplitude of 0.025 is about 50% of that originally predicted and used for the design of the OPTR. Why the OPTR exceeded the predicted performance in spite of the lower pressure amplitude still needs further investigation. It is possible that the regenerator loss in a large void volume may be reduced at such low pressure ratios.

CONCLUSIONS AND FURTHER WORK

The first cryocooler with no moving parts was constructed and its overall performance exceeded design calculations. The lowest temperature reached was 90 K. A refrigeration power of 5 W at 120 K was achieved with 3 kW of heat input to the TAD.

The first-generation TAD shows considerable promise for meeting requirements for SDIO satellite cryocoolers, but much work remains to be done. Future work will be directed toward improving efficiency, mass, and size. Specific investigations will include tests to determine the effects of geometry, such as resonator loop coiling, honeycomb stacks, and spherical resonator ends. Also, heat losses and energy balances, advanced materials, vibration reduction, turbulence effects, and heat exchangers will be studied for ways to improve the existing TAD.

Future plans for improvement of the OPTR will be directed toward optimizing its volume relative to the TAD. Larger OPTR systems will produce greater refrigeration power for the same pressure amplitude. Other sizes of OPTR systems will be tested to determine the optimum volume ratios. The behavior of regenerators at low pressure ratios will be investigated using numerical modeling to help in optimizing their design. Varying the geometry of the regenerator matrix also offers potential for improved performance. With improved regenerator performance, frequencies up to 100 Hz may be possible, allowing the resonator tube of the TAD to be shortened considerably.

ACKNOWLEDGEMENTS

The authors are grateful to Eric Marquardt of NIST for assistance in constructing the OPTR and to Robert Ortega of LANL for assistance in constructing the TAD and in performing many of the tests with the TADOPTR.

Table 3. TADOPTR temperatures and pressure ratios during normal operation.

TAD power (kW)	Hot end stack temperature (K)	Minimum OPTR temperature (K)	Pressure ratios, P_H/P_L		
			TAD	Regenerator	Pulse tube
2.0	868	98.0	1.0686	1.0638	1.0360
2.5	908	94.1	1.0793	1.0718	1.0394
3.0	950	91.0	1.0918	1.0813	1.0485
3.0	926	119.5 @ 5 W	1.0954	1.0870	1.0517

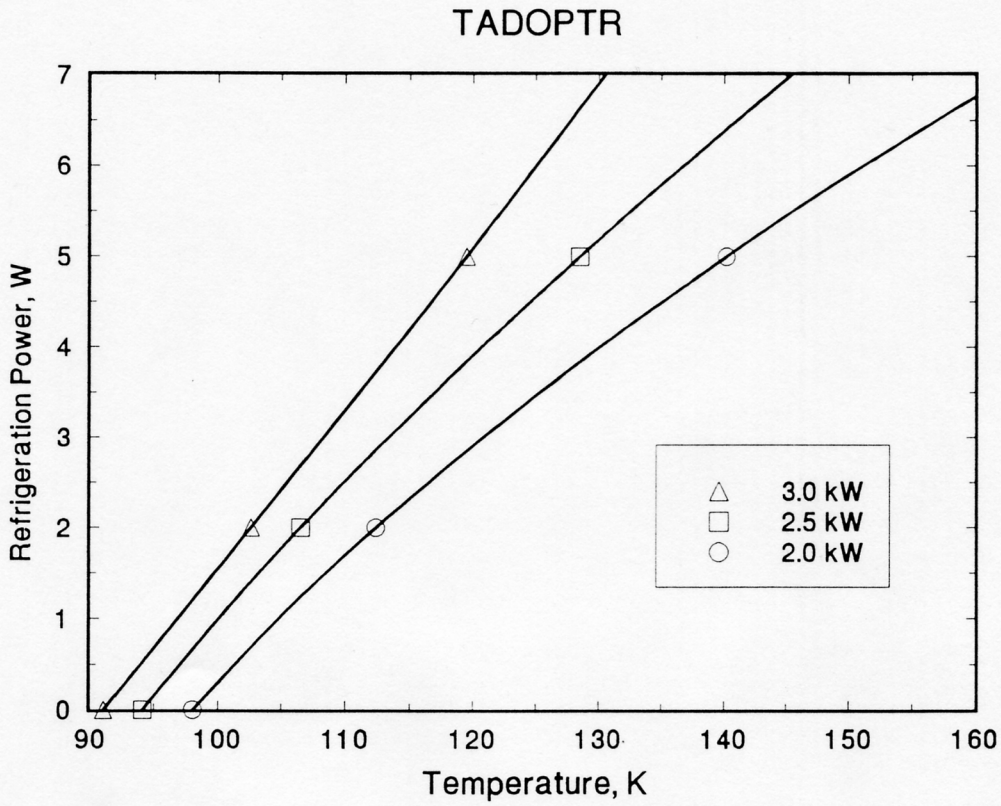

Fig. 7. Refrigeration power of the TADOPTR with several power inputs to the TAD.

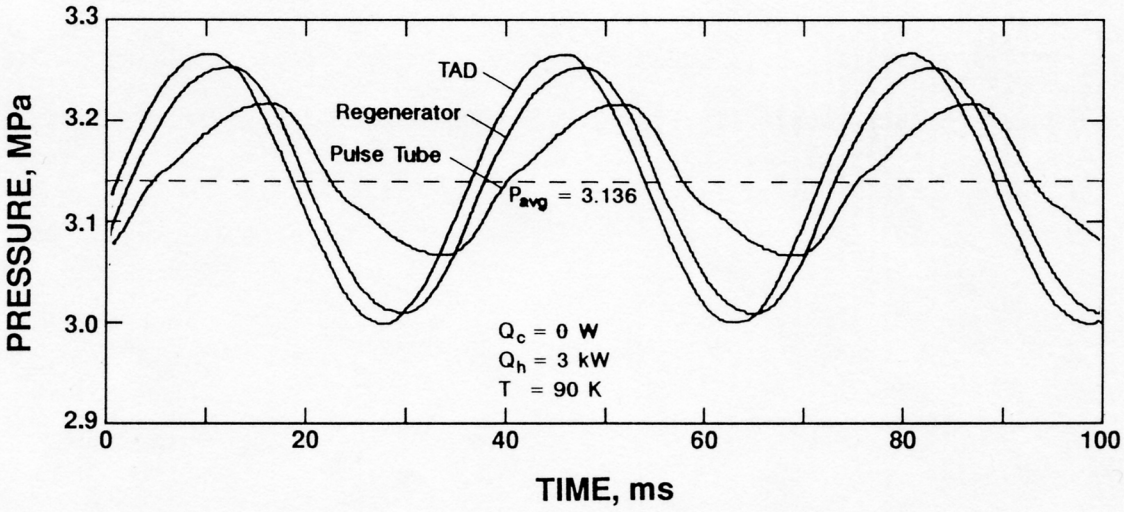

Fig. 8. Instantaneous pressure at three locations in the TADOPTR during normal operation.

REFERENCES

[1] R. Radebaugh, "Pulse tube refrigeration--a new type of cryocooler," *Japanese J. Appl. Phys.*, vol. 26, suppl. 26-3 (1988) p. 2076.

[2] R. Radebaugh, "A review of pulse tube refrigeration," in: *Advances in Cryogenic Engineering*, vol. 35B (1990) p. 1191.

[3] J. Wheatley and A. Cox, "Natural engines," *Physics Today*, vol. 38, no. 8 (1985) p. 50.

[4] J.A. Angelo, Jr. and D. Buden, *Space Nuclear Power*, Orbit Book Company, Malabar, FL (1985).

[5] G.W. Swift, "Thermoacoustic engines," *J. Acoust. Soc. Am.*, vol. 84(4) (1988) p. 1145.

[6] W.L.M. Nyborg, "Acoustic streaming," in: *Physical Acoustics*, W.P. Mason, ed., vol. 2B, Academic Press, N.Y. (1965) p. 265.

[7] P.J. Storch and R. Radebaugh, "Development and experimental test of an analytical model of the orifice pulse tube refrigerator," *Advances in Cryogenic Engineering*, vol. 33 (1988) p. 851.

[8] R. Radebaugh and S. Herrmann, "Refrigeration efficiency of pulse tube refrigerators," *Proc. 4th Int'l Cryo. Conf.*, Easton, MD (9,1986) p. 119.